

Argon/humid air plasma chemistry: focus on gas phase reaction kinetics

W. Van Gaens, A. Bogaerts

Research group PLASMANT, Department of Chemistry, University of Antwerp, Antwerp, Belgium

Abstract: We developed a zero-dimensional semi-empirical model to describe the gas phase kinetics in an argon plasma jet flowing into humid air. The model includes an extended plasma chemistry set of 84 different species and 1885 reactions. The density profiles of the biomedically active species are presented for a typical plasma jet device, and the effects of O₂, N₂ or H₂O admixtures to the argon feed gas are investigated.

Keywords: plasma medicine, chemical kinetics model, plasma jet, humid air, argon

1. Introduction

Plasma medicine is a research area of growing interest. For improving the field, however, a good insight in the underlying mechanisms is required. For instance, the complex chemical processes occurring in a plasma jet flowing into the ambient air, need to be better understood. For this purpose, we make use of a zero-dimensional chemical kinetics model, that takes into account a large number of different plasma species and chemical reactions, as will be explained in Section 2. Typical calculation results, such as the density profiles of the biomedically active plasma species, and the influence of O₂, N₂ or H₂O admixtures to the argon feed gas, will be presented in Section 3. Finally, a conclusion will be given in Section 4.

2. Description of the model

We make use of the zero-dimensional model, GLOBALKIN, developed by M. Kushner and coworkers [1]. This model consists of three basic modules, i.e., a 0D plasma chemistry module, a Boltzmann equation module and a circuit module, but in this work, only the first two modules are used.

The time-evolution of the species densities is calculated, based on production and loss processes, as defined by the chemical reactions:

$a_{ij}^{(1)}$ and $a_{ij}^{(2)}$ are the stoichiometric coefficients of species i , at the left and right hand side of the reaction j , respectively. N_i is the species density at the left-hand side of the reaction, and k_j is the rate coefficient of reaction j .

The electron temperature is calculated with the following energy balance equation:

N_e is the electron density, T_e is the electron temperature, and j_e and E are the electron current density and electric field in the plasma, ν_{mi} is the electron momentum transfer

collision frequency with species i , m_e is the electron mass, and M_i and T_i are the mass and temperature of species i . k_1 is the reaction rate coefficient of electron impact reaction 1, N_1 is the density of species 1, and $\Delta\epsilon_1$ is the change in electron energy (hence negative value for electron energy loss). The first term at the right-hand side of this equation is the energy gain due to Joule heating, whereas the second and third terms denote the energy losses due to elastic and inelastic collisions, respectively. As the model is 0D, we don't know the electric field distribution in the plasma; therefore, the Joule heating term is determined by an estimated power density, used as input in the model (see below).

The model includes 84 different plasma species. Special emphasis is put on all possibly important biomedically active species, like N, O, OH, O₂(¹ Δ_g), O₃, OH, H₂O₂, NO_x, HNO_x, O₂⁻, etc. Most of them are identified as possibly important reactive oxygen species (ROS) and reactive nitrogen species (RNS), as reported in a recent review by Graves [2]. These species are assumed to react with each other in 1885 reactions, i.e., 278 electron impact and 1596 heavy particle collisions. All details about the species included and the full reaction chemistry set can be found in [3]. Moreover, this paper also presents two reduced chemistry sets, that can be used for 2D or 3D modeling.

The 0D model had to be modified to mimic the experimental conditions of the plasma jet under study (see below). Indeed, there exist many different plasma jet configurations, which differ from each other in the way of power deposition, the position of the plasma jet nozzle exit, the speed of humid air diffusion into the noble gas stream, different gas flow speeds, etc., and all these aspects influence the chemistry significantly. Therefore, in this paper the operating conditions are chosen similar as for the argon plasma jet device developed at Eindhoven University of Technology by P. Bruggeman and coworkers [4]. A photograph of this jet, freely propagating in an open air atmosphere, is shown in Fig. 1 (upper panel).

To mimic the experimental conditions, several parameters, such as the gas temperature evolution along the plasma jet symmetry axis, the admixture speed of the

surrounding humid air atmosphere into the noble gas effluent, the power deposition profile and the gas flow speed, are fitted to experimental and modelling data. In this way, our model is used in a semi-empirical way. More details about this approach can be found in [3].

Although the model is 0D, it could be used to calculate the plasma quantities as a function of distance along the plasma jet symmetry axis, i.e., by assuming a 'pseudo-one-dimensional plug flow'. Indeed, this makes it possible to translate the time dependent evolution of species densities, as calculated in the 0D model, into results as a function of the position in the plasma jet device and effluent. In this approach, we assume that the tube of the plasma jet device, the plasma jet itself and the afterglow region in the far effluent can be represented by a long cylinder (see Fig. 1), where constant atmospheric pressure conditions apply. The magnitude of the flow velocity determines the change of position of a volume averaged (0D) plug flow element, i.e. a cylindrical segment, along the jet stream. In our approach, we assume that axial transport of mass and energy due to drift and concentration gradients is negligible in comparison to axial transport by convection. Also, species transport in the radial direction is not included self-consistently in the model. We expect that this is acceptable, due to the very high axial flow speed in the first few cm's after the nozzle exit. Further details about this approach can be found in [3].

Our model was validated with experimentally measured absolute ozone density profiles, and good qualitative and even reasonable quantitative agreement was reached [4].

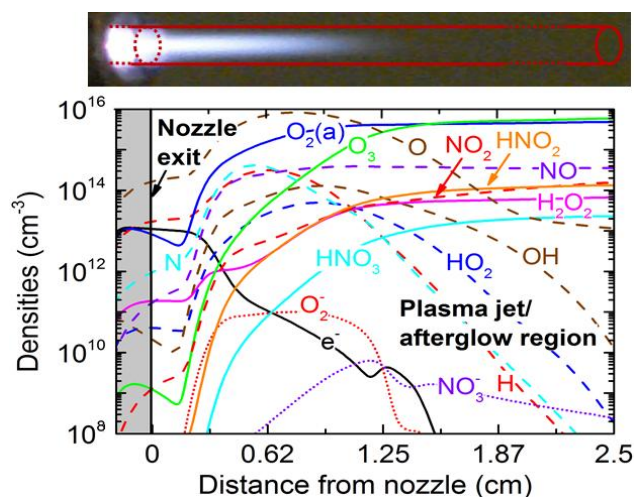


Fig. 1 Photograph of the plasma jet under study [4], propagating freely in open air atmosphere (upper figure), and calculated densities of biomedically active species along the symmetry axis of the plasma jet (lower figure). The interior of the plasma jet device is represented by the grey area, beginning at the needle electrode tip until the nozzle exit (indicated with axial position = 0 cm). Radicals are indicated by a dashed line, whereas ions are represented by a dotted line.

3. Results and discussion

3.1. Basis case study

In this section, calculation results are presented for a basic case, i.e., 2 slm gas feed, 6.5 W total deposited power and 50% relative humidity of the ambient air. No air components were admixed into the argon feed gas, although some typical air impurity levels (about 10 ppm) are assumed to be present.

The calculated density profiles of the biomedically important plasma species are plotted along the plasma jet axis in Figure 1. The grey area indicates the interior of the plasma jet device. The nozzle exit is indicated at axial position = 0 cm, and it is followed by the zone where the plasma jet propagates into ambient air. Around 1.2 cm from the nozzle exit, the plasma jet becomes an afterglow.

Figure 1 illustrates that oxygen, hydrogen and nitrogen radicals are already formed within the device in large quantities (about 10, 1 and 0.1 ppm, respectively), thus about 50% of the molecular oxygen is dissociated. This is consistent with the $O_2(a)$ density profile which is decreasing up to 0.25 cm behind the nozzle exit, since ground state oxygen is largely depleted.

At a distance of 0.25 cm from the nozzle exit, the effects of ambient air diffusion start to influence the density profiles significantly. The diffusion is non-linear, which can, among others, be explained by the deceleration of the jet stream. It is clear from Figure 1 that the densities of all biomedically active plasma species increase strongly from this point. The highest density is reached by atomic oxygen at 0.8 cm. Because power density and gas temperature are decreasing along the effluent, the electron density and dissociation degrees cannot be maintained, while the rate of association reactions (e.g., $O + O_2 + M \rightarrow O_3 + M$) increases. As a result, the O atoms are mainly converted into ozone, which becomes the dominant species in the far effluent.

Note, on the other hand, that ozone is also destroyed by atomic oxygen at slightly elevated temperatures by the following reaction: $O + O_3 \rightarrow O_2 + O_2$.

Other important radicals formed in the afterglow region are N, H, OH, HO_2 and NO. The latter is a relatively stable species in the gas phase, but the other radicals are quenched much more quickly than the O atoms. They are easily converted into 'long living' species such as NO_2 , H_2O_2 , HNO_2 and HNO_3 . Note that the timescales (at flow speeds of up to $3000 \text{ cm}\cdot\text{s}^{-1}$) in these simulations are in the order of milliseconds, whereas the timescales can be much larger in stationary systems. In that case, further reactions might take place, e.g. reactions between ozone and different NO_x species:

- $O_3 + NO \rightarrow NO_2 + O_2$,
- $O_3 + NO_2 \rightarrow NO_3 + O_2$,
- $O_3 + NO_3 \rightarrow O_2 + O_2 + NO_2$, etc.

The negatively charged species are formed through dissociative attachment, mainly:

- $O_2 + e^- \rightarrow O^- + O$
- $H_2O + e^- \rightarrow H^- + OH$

By means of association or charge transfer reactions with neutrals, high O_2^- densities and later in the effluent high NO_3^- densities are formed. The electron density drops quickly in the afterglow due to air diffusion, and eventually all negative charge is present in the form of anions.

The positive ion densities are balancing the total negative charge density since charge neutrality is assumed. Our calculations reveal that as soon as the air concentration in the jet becomes significant, the positive ions are almost immediately clustering with water. Hence, the water clusters, i.e., $H_3O^+ \cdot (H_2O)_x$, quickly become the most important charge carriers throughout the jet effluent. Their densities are illustrated in Figure 2. It is clear that the clusters keep increasing in size as a function of distance from the nozzle. All water clusters, regardless of their size, recombine with electrons and anions (O^- , O_2^- , NO_3^- , depending on their densities as a function of the distance), causing a gradual decrease in the total amount of positive and negative ions of about three orders of magnitude within 2 milliseconds.

For a more detailed discussion about the important plasma species and their chemical pathways, we refer to [3].

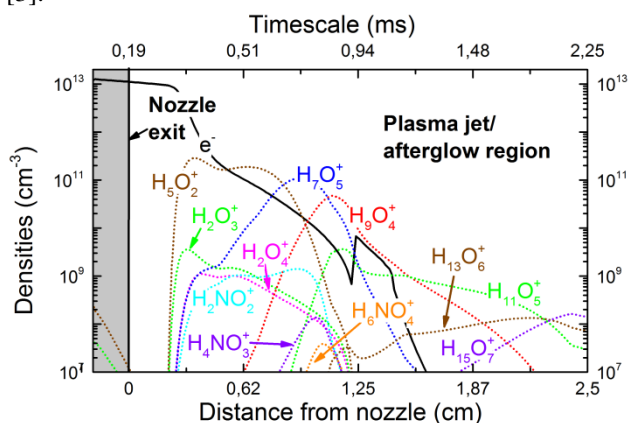


Fig. 2 Calculated densities of the ionic water clusters along the symmetry axis of the plasma jet. Note that the time and distance dimensions (i.e., upper and lower x-axis, respectively), are correlated with an externally calculated velocity profile.

3.2. Air component admixtures to the argon feed gas

In this section the influence of O_2 , N_2 or H_2O admixtures to the argon feed gas is investigated for several biomedically active species. The operating conditions are the same as in previous section, except that 1% of O_2 , 2% dry air (1/1 ratio O_2 and N_2) or 1% of H_2O are added to the argon gas.

Figure 3 illustrates the calculation results for the electron densities, as well as for the density profiles of several other important plasma species, in the basic case (no admixtures) and in the 3 cases mentioned above.

The electron density is initially much lower when admixtures are used. Indeed, in these cases a higher

amount of electronegative species is formed and hence the electron attachment rates increase. However, after a distance of 0.5 cm from the nozzle exit, the electron density profile becomes similar in all four cases, as the air impurity level becomes the same, due to ambient air diffusion.

As expected, the O, N and OH radicals are formed in much greater quantities when the corresponding molecular species (O_2 , N_2 and H_2O) is admixed into the feed, although the electron density is lower for a large part of the jet. This is because the drop in electron density is less than two orders of magnitude, while the admixture results in a density increase of a factor 10^3 for oxygen and nitrogen and even 10^4 for water. Thus, the absolute electron impact dissociation rates still increase.

The ozone formation is clearly less efficient in the case of water admixture, because of two reasons: oxygen radicals are partially consumed by OH, forming HO_2 , and moreover, ozone is efficiently destroyed by H. Both OH and H have a higher density in the case of the water admixture. Eventually, HO_2 and OH lead to hydrogen peroxide, which explains the high density of the latter under these conditions. Naturally, the ozone density is much higher when molecular oxygen is admixed. There is, however, little difference between the cases with or without nitrogen, as it seems not to increase the formation of components that can destroy ozone (NO_x).

Finally, in the far effluent the density profiles of both NO and HNO_3 are not very much affected by the different admixtures. Of course, the NO formation is initially higher in the case of the O_2/N_2 admixture but eventually the gas composition only differs by maximum a factor of 2 for the different conditions.

4. Conclusions

We have demonstrated, by means of 0D chemical kinetics modeling, how the densities of biomedically active species evolve throughout a plasma jet and the afterglow region, for an argon plasma jet flowing into humid air. $O_2(a)$, O_3 , H_2O_2 , NO, NO_2 , HNO_2 and HNO_3 are identified as long living species, at least for the simulated timescales. Radicals such as O, N, H, HO_2 and OH are more rapidly quenched. The treatment distance can therefore be utilized to obtain the desired species cocktail. The latter can be further modified by adding specific admixtures with well-defined concentrations.

5. Acknowledgements

We would like to acknowledge the Institute for the Promotion of Innovation by Science and Technology in Flanders (IWT Flanders) for financial support, P. Bruggeman and co-workers at Eindhoven University of Technology for providing experimental data, and M. Kushner and co-workers for providing the GLOBALKIN code.

6. References

- [1] R. Dorai, M. J. Kushner, *J. Phys. D: Appl. Phys.* 36, 1075 (2003).
 [2] D. B. Graves, *J. Phys. D: Appl. Phys.* 45, 263001 (2012).

- [3] W. Van Gaens, A. Bogaerts, *J. Phys. D: Appl. Phys.* (2013) in press.
 [4] S. Zhang, W. Van Gaens, B. Van Gessel, S. Hofmann, E. van Veldhuizen, A. Bogaerts, P. Bruggeman, *J. Phys. D: Appl. Phys.* 46, 205202 (2013).

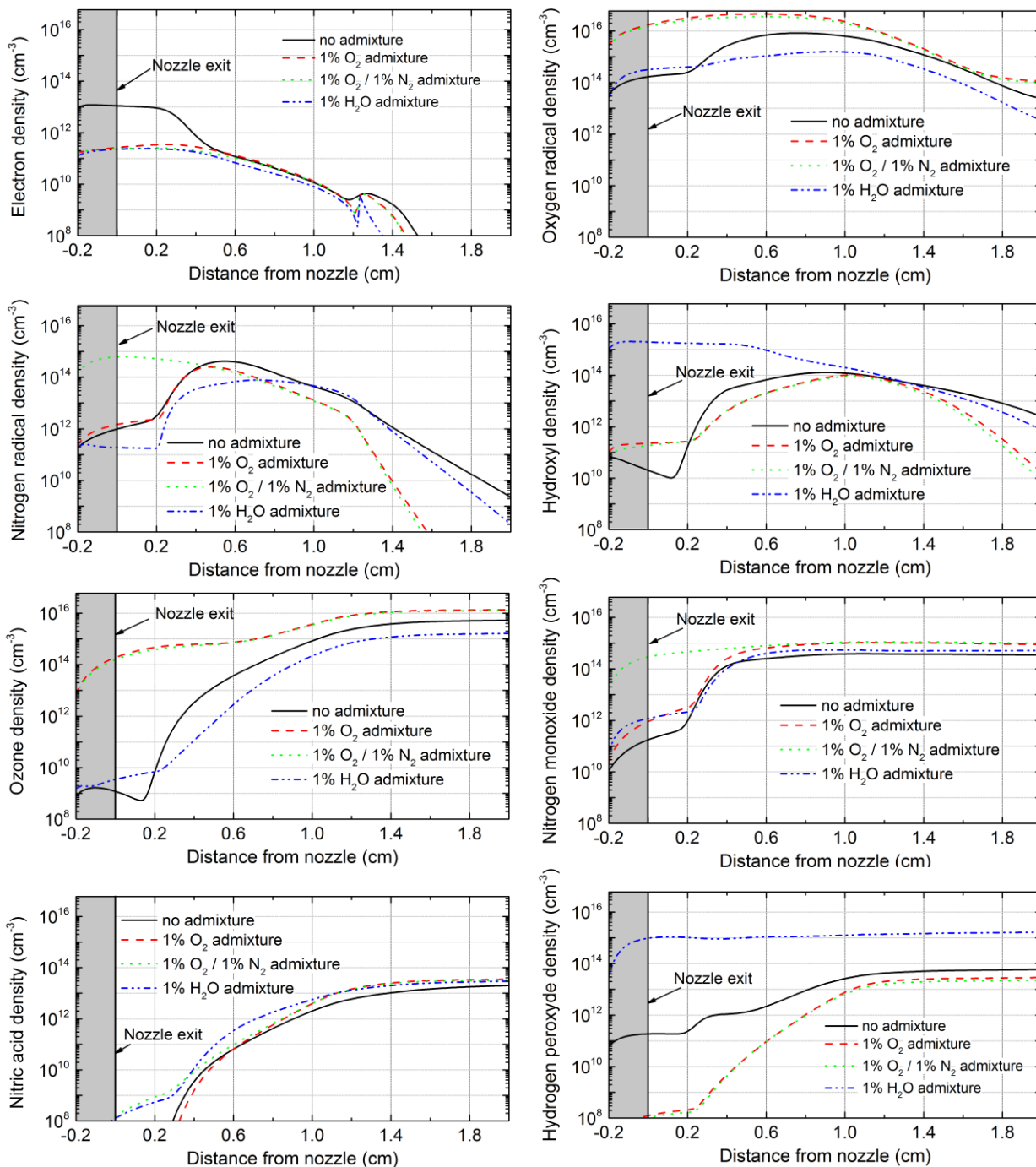


Fig. 3 Calculated density profiles along the symmetry axis of the plasma jet of electrons, oxygen radicals (O), nitrogen radicals (N), hydroxyl (OH), ozone (O_3), nitrogen monoxide (NO), nitric acid (HNO_3) and hydrogen peroxide (H_2O_2), respectively, for different air component admixtures to the argon gas feed (see legends).